

Ru-doping-induced ferromagnetism in charge-ordered $\text{La}_{0.4}\text{Ca}_{0.6}\text{MnO}_3$

C. L. Lu, X. Chen, S. Dong, K. F. Wang, H. L. Cai, and J.-M. Liu*

Laboratory of Solid State Microstructures, Nanjing University, Nanjing 210093, China

and International Center for Materials Physics, Chinese Academy of Science, Shenyang 110016, China

D. Li and Z. D. Zhang

Shenyang National Laboratory for Material Science, Institute of Metal Research, Chinese Academy of Sciences, Shenyang 110016, China

(Received 24 February 2009; revised manuscript received 2 May 2009; published 4 June 2009)

Impurity effects on the stability of a charge-ordered antiferromagnetic state in electron-doped manganite $\text{La}_{0.4}\text{Ca}_{0.6}\text{MnO}_3$ are investigated by doping Ru for Mn. Our results show that Ru doping at a tiny level of $\sim 2\%$ is sufficient to suppress significantly the charge-ordered insulated state and generate a ferromagnetic metallic one. The blocked metastable state and the first-order metal-insulator transitions observed in the slightly doped samples can be attributed to the phase-separated state where ferromagnetic domains are embedded in the charge-ordered matrix. The doping effect is further investigated theoretically based on the two-orbital model. The calculation suggests that two factors are vitally important for the Ru-doping driven strong ferromagnetic tendency: (1) the ferromagnetic coupling between Ru and Mn spins and (2) the enhancement of e_g electron density while the topological defects always contribute to the instability of charge-ordered state.

DOI: 10.1103/PhysRevB.79.245105

PACS number(s): 75.47.Lx, 75.47.Gk, 71.30.+h

I. INTRODUCTION

Charge-ordered (CO) states are essential ingredients of the physics of colossal magnetoresistance (CMR) in manganites $\text{RE}_{1-x}\text{AE}_x\text{MnO}_3$, where RE is the rare-earth element and AE the divalent alkaline-earth element.¹⁻³ In the past years, much attention has been attracted on the phase transitions from the CO state to the FM metallic state or others. These phase transitions, which are usually accompanied with prominent physical properties changes, can be achieved by applying magnetic field⁴ or electric field,^{5,6} or introducing the A-site disorder,⁷⁻¹⁰ or preparing these CO manganites to nanosized forms.¹¹⁻¹³ Recently, intensive experimental and theoretical interests have been guided toward the B-site doping effects in CO manganites due to the fact that the physical properties of the CO state can be tuned in a large scale by low-level B-site doping.¹⁴⁻²² The B-site substitution in CO manganites causes a lot of interesting phenomena such as phase separation (PS),²³⁻²⁶ metal-insulator transition (MIT) of first-order nature,²⁷⁻²⁹ ultrasharp metamagnetic transition,^{30,31} and novel dynamical effects.³²⁻³⁴

Generally, the B-site doping in CO manganites may lead to three straightforward effects: (i) topological defects which always frustrate the long-range charge ordering;^{14,31} (ii) tuning of e_g charge density;³⁵ and (iii) direct-exchange coupling with Mn cations if the doping cations have finite magnetic moments, such as Cr^{3+} or Fe^{3+} .^{28,29} It seems that all of the three kinds of consequences destabilize the CO state. For effect (ii), an increase in e_g charge density favors the FM phase and a reduction does not. In consequence, such a doping seems always to lead to phase-separated electronic structure. In fact, recent experiments showed that the CE-type CO state can be broken and weak FM tendency can emerge even by tiny nonmagnetic substitutions, such as Al^{3+} and Ga^{3+} , although the reduction in e_g electron is disadvantageous to FM phase.^{14,31} A higher valence (+4 or +5) doping will be efficient in enhancing the FM stability over the CO state because of effect (i) suppressing the CO state and effect and

(ii) favoring the FM tendency. Clearly, effect (iii) is also included if the doping is with magnetic ions of valence higher than +3 and one may expect even more significant suppression of the CO state and enhancement of the FM state.

On the other hand, recently, Şen *et al.*^{36,37} claimed theoretically that a short-range CO antiferromagnetic (AFM) state is needed as a competitor of FM metal phase for a complete rationalization of CMR physics and the true CMR effect ensues at the phase boundary between FM metal and CO-AFM state. It is thus interesting to check this theoretical prediction of Şen *et al.* by tuning the instability of highly stable CO state with B-site doping, excluding the high sensitivity of the critical region of phase diagram at $x \sim 0.5$.⁷⁻¹⁰

Following these arguments, we choose $\text{La}_{0.4}\text{Ca}_{0.6}\text{MnO}_3$ as prototype sample to investigate the B-site doping effects. First, electron-doped manganite $\text{La}_{0.4}\text{Ca}_{0.6}\text{MnO}_3$ exhibits robust charge-ordered state which is accompanied by co-existed C-type and CE-type AFM spin orderings.² With respect to the critical-state manganites at $x \sim 0.5$, the CO state of this compound is much more stable but less sensitive to intrinsic or external stimuli, such as A-site disorder or magnetic field up to several tesla.³ Therefore, $\text{La}_{0.4}\text{Ca}_{0.6}\text{MnO}_3$ can provide an ideal arena to highlight the genuine B-site doping effect in CO manganites. Second, the doping species we choose is Ru which allows for the simultaneous activation of the three effects (i)–(iii) because Ru cations have high valence and also magnetic species.¹⁸⁻²¹ The overlapping of the three effects enables significant impact on the instability of the CO state even at a tiny Ru doping level. In addition, we are allowed with the opportunity to check the theoretical prediction for the origin of a true CMR effect^{36,37} without much worrying about the high sensitivity encountered for those manganites at $x \sim 0.5$.

In this paper, we investigate the B-site effects on structure, transport, and magnetic properties of $\text{La}_{0.4}\text{Ca}_{0.6}(\text{Mn}_{1-y}\text{Ru}_y)\text{O}_3$ with low Ru-doping levels at the B-site ($0 \leq y \leq 0.07$). The robust CO-AFM insulated phase in

the adopted compound is significantly suppressed and FM metallic state is generated. This *B*-site doping effect is further studied by theoretical calculation, which reveals consistency with our experimental results. The remainder of this paper is organized as follow. We report the sample preparation and property characterizations using various techniques in Sec. II. The details of the measured data are presented in Sec. III, where we discuss every aspect of the doping effects in $\text{La}_{0.4}\text{Ca}_{0.6}(\text{Mn}_{1-y}\text{Ru}_y)\text{O}_3$ ($0 \leq y \leq 0.07$), and give a comparison between the theoretical calculation and experimental results. A short summary is given in Sec. IV.

II. EXPERIMENTAL PROCEDURE

A series of polycrystalline samples $\text{La}_{0.4}\text{Ca}_{0.6}(\text{Mn}_{1-y}\text{Ru}_y)\text{O}_3$ ($0 \leq y \leq 0.07$) were prepared by conventional solid-state reaction in air. The highly purified powders of oxides carbonates were mixed in stoichiometric ratios, ground, and then fired at 1200 °C for 24 h in air. The resultant powders were reground and pelletized under 3000 psi pressure to disks of 2 cm in diameter; then the pellets were sintered at 1300 °C for 24 h in air. X-ray diffraction (XRD) with Cu $K\alpha$ radiation was performed on these samples at room temperature (T).

The magnetic properties as a function of T and H were measured using Quantum Design superconducting quantum interfering device (SQUID). In the zero-field-cooled (ZFC) measurements the samples were cooled from to 5 K under zero magnetic field and then the magnetization (M) were measured in the warming process with a field of $H = 100$ Oe. The field-cooled (FC) measurements were performed under a field of $H = 100$ Oe when sample was cooled from 300 to 5 K. For the field-cooled-warming (FCW) cases, samples were first cooled from 300 to 5 K under a field of $H = 100$ Oe, and then M was measured in the warming process under the same field. The hysteresis loops were recorded at 5 K from $H = 0$ to 6 T after the ZFC sequence. The transport properties were measured using a standard four-probe method down to 5 K with/without magnetic field using a cryogen-free low T high magnetic-field system.

III. RESULTS AND DISCUSSION

A. Crystal structure

First, we need to check the crystal-structure dependence on the Ru doping, and at the clean limit no such a dependence is preferred. In Fig. 1 we present the XRD patterns measured at room T for a series of samples with different Ru levels $0 \leq y \leq 0.07$. All the samples are well crystallized with pure orthorhombic structure of space group $Pbnm$. No identifiable reflection shift upon change in doping level is observed, demonstrating no change in the crystallographic structure and lattice constant on variance of y . To further confirm this fact, we perform the Rietveld refinement on the diffraction spectra. The data on sample $y = 0.07$ are shown in Fig. 1(b). Only very small difference between the measured spectrum and refined one can be identified. The reliability of the Rietveld refinement is demonstrated by the high-quality refinement parameters $R_{wp} = 11.16\%$ and $R_p = 7.78\%$ for

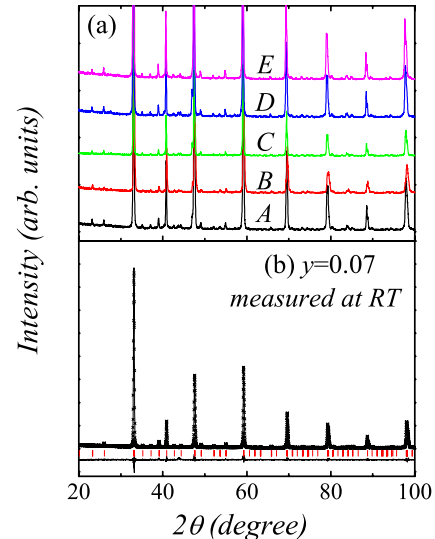


FIG. 1. (Color online) (a) X-ray diffraction θ - 2θ spectra at room temperature for a series of samples of variance y (from bottom to top): (A) $y = 0$; (B) $y = 0.02$; (C) $y = 0.03$; (D) $y = 0.05$; and (E) $y = 0.07$. (b) Rietveld refinements for sample $y = 0.07$. The cross points and solid line represent the experimental data points and the Rietveld refined result, respectively. The lower rows of markers indicate the positions of structure reflections. The difference is shown on the bottom as solid line.

sample $y = 0$, and $R_{wp} = 8.59\%$ and $R_p = 6.25\%$ for sample $y = 0.07$. The lattice constant at room temperature as obtained by the refinement are $a = 5.3977(1)$ Å, $b = 5.4133(1)$ Å, and $c = 7.6092(1)$ Å for sample $y = 0$. For sample $y = 0.07$, they are $a = 5.4017(1)$ Å, $b = 5.4004(1)$ Å, and $c = 7.6173(1)$ Å. It is revealed that the lattice parameters show little variation upon increasing y and the volume change between samples $y = 0$ and $y = 0.07$ is only $\sim 0.5\%$ and less.

B. Transport properties

We subsequently measure the temperature dependences of resistivity ρ for all samples under various external magnetic fields to demonstrate the doping effect. In general, one sees an overall decrease in ρ with increasing y . For sample $\text{La}_{0.4}\text{Ca}_{0.6}\text{MnO}_3$ ($y = 0$), ρ shows a typical insulated behavior over the whole T range, as shown in Fig. 2(a) and the value of ρ only shows a small change ($< 1\%$) under a high magnetic field $H = 9$ T, demonstrating the high robustness of the CO (AFM) state. However, a doping as low as $y = 0.02$ was found to be sufficient to destabilize the CO state. In Fig. 2(b) the data are given at $y = 0.02$. First, a clear MIT at $T = T_{\text{MI}} = 71$ K and the resistivity at $T = 2$ K is 4 orders of magnitude lower than that at $y = 0$. Second, significant MR effect is demonstrated by comparing the low T resistivities at $H = 0$ and 6 T. With increasing y , T_{MI} increases rapidly from 71 to 132 K and becomes saturated at $y = 0.05$ and 0.07, as shown in Figs. 2(c) and 2(d). Resistivity ρ shows a continuous decrease but the MR effect at low T falls down with respect to the case of $y = 0.02$. The relationship between T_{MI} and y is plotted in the inset in Fig. 2(d), where T_{MI} increases quickly

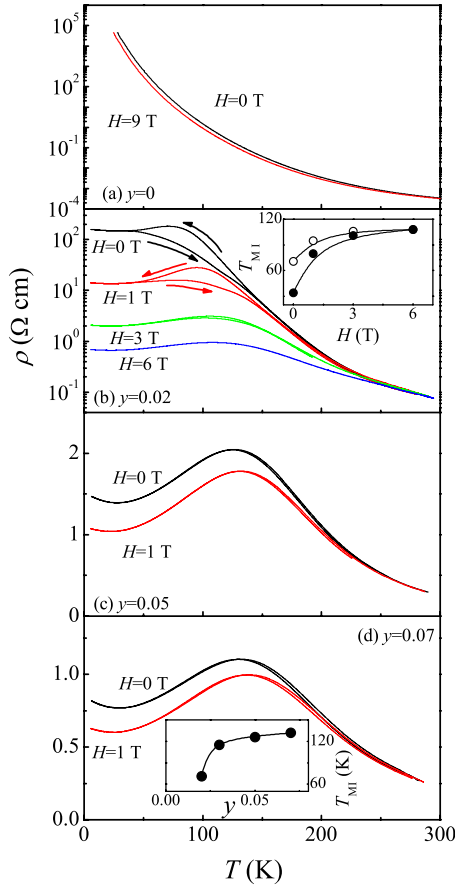


FIG. 2. (Color online) Temperature profiles of resistivity at various external magnetic fields for samples of (a) $y=0$; (b) $y=0.02$; (c) $y=0.05$; and (d) $y=0.07$, respectively. The inset of (b) shows T_{MI} of sample $y=0.02$ for both cooling (open circle) and warming (solid circle) cases as a function of magnetic field H . The inset of (d) shows T_{MI} of the cooling case as a function of y , the black line is guide for the eyes.

with y at $y < 0.05$, and then becomes saturated upon y increasing to 0.07.

Here, it should be addressed that for $y=0.02$, the T dependence of ρ exhibits distinct hysteresis (uses arrow to label the cooling/warming sequences), often identified in the phase-separated manganites and regarded as an indication of a first-order transition,³⁸ demonstrating that the electronic structure is a PS state with coexisting FM phase and CO phase, to be further confirmed below by the magnetization data. Nevertheless, the hysteresis behavior becomes much weaker at $y=0.05$ and even negligible at $y=0.07$, indicating serious suppression of the first-order phase transitions. At the first glance, these facts lied in the magnetotransport data allow us to develop a one-to-one correspondence between the MR effect and the PS state: a well-developed PS state benefits to the large MR effect and thus to confirm the prediction of Şen *et al.*: *the CO (AFM) state is needed as a competitor of FM metal phase for a complete rationalization of CMR physics.*

Looking at the effect of external field, as shown in Fig. 2(b) at $y=0.02$, one finds that the first-order transitions can be suppressed, reflected by the reduction in hysteresis width. The T_{MI} - H relationship, for both the cooling and warming

processes, is plotted in the inset of Fig. 2(b). T_{MI} shifts toward high T side and eventually becomes saturated with increasing H . These features indicate the crossover behavior from the first-order transition to the second one. This H dependence is understandable because in manganites, the first-order transition point can be shifted by magnetic field but the second one is not sensitive.³⁸

C. Magnetic behavior

The above magnetotransport data do reveal a remarkable effect of the Ru-doping at a tiny level and do confirm the theoretical prediction on the CMR physics, as addressed in Sec. I. However, additional evidence from other aspects is obviously necessary.

In addition to the significant response of the magnetotransport behavior to the doping, the response of the magnetization behaviors is remarkable too. Figure 3 presents the measured M as a function of T for the ZFC, FC, and FCW cases, respectively. Again for a first glance, the 2% Ru doping enhances M for more than 2 orders of magnitude with respect to sample $y=0$, again demonstrating the colossal effect of Ru-doping. In details, for sample $y=0$, a broad peak at $T=T_{CO}=260$ K indicates the charge-ordering transition. The AFM transition is normally indicated by a much weaker feature at $T=T_N=140$ K, although it is not clearly visible on the present scale. As further cooling to ~ 50 K, the magnetization shows a slight rebounding, indicating a canted AFM ground state.^{2,39}

For sample $y=0.02$, the CO state is partially suppressed and T_{CO} shifts downward to ~ 200 K, as shown in Fig. 3(b). Below T_{CO} , a clear FM transition is evidenced at $T=T_C=125$ K (T_C was determined using the Lorentzian function fit of the derivation curve of the ZFC/FCW case). Upon further cooling, M increases quickly to a maximum at $T \sim 70$ K, and a divarication arises between ZFC and FCW cases at this point. An evident hysteresis between the FC and ZFC/FCW cases, similar to the transport behavior, is evidenced. The value of M at the ZFC mode is even larger than that at the FC mode in the range $70 < T < 140$ K. Both features suggest that the system is blocked into a metastable state, a clear feature of the first-order transition and PS state.⁴⁰

Further increase in the doping level to $y=0.05$ and 0.07 results in continuous enhancement of M over the whole T range, indicating the preference of the FM phase in competition with the CO phase. The transition point T_C rapidly increases from 120 to 260 K. Going into details of the case $y=0.05$, it is found that the ZFC data show clear AFM background and peaked feature at $T=240$ K is identified while the FC data evidence a broad FM transition beginning at $T \sim 260$ K. For $y=0.07$, no more visible feature associated with the CO (AFM) phase is probed although it does not mean disappearance of the CO phase in the sample.

Going deeper into the dynamics of magnetization, the H dependence of M at $T=5$ K for all doped samples are shown in Fig. 4. Our previous results revealed that the M - H curve of sample $y=0$ is very thin and does not show any saturation as H is as large as 3 T.³⁹ However, for $y=0.02$, the measured

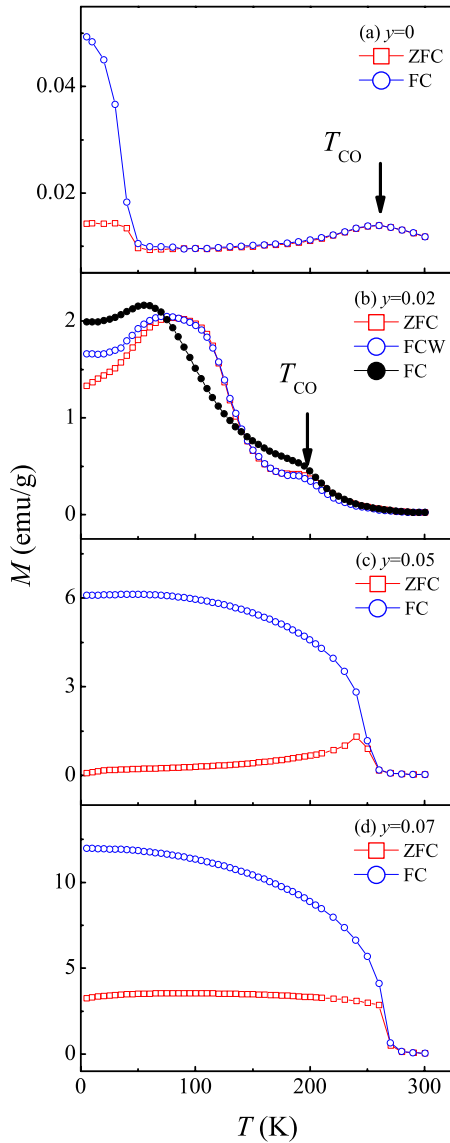


FIG. 3. (Color online) Temperature profiles of magnetization at $H=100$ Oe for sample of (a) $y=0$; (b) $y=0.02$; (c) $y=0.05$; and (d) $y=0.07$, respectively. Measurements were performed in both cooling and warming runs.

M is much larger than the undoped sample and easily reaches a saturated value. A typical feature of metamagnetic transition can be seen.⁴¹ To understand this metamagnetic state, we analyze in details the dynamics of magnetization. In the low-field range, M shows a sharp increase with increasing H , associated with the alignment of the FM domains, and the obtained total moment of these FM domains is about $0.66\mu_B$ per unit. It is known that the high-spin Mn gives spin-ordered moment $\mu = gs\mu_B$ (orbital contribution quenched), where Mn^{3+} and Mn^{4+} carry $4\mu_B$ and $3\mu_B$, respectively. Taking the moment of Ru ions into account, the estimated spontaneous FM volume fraction in sample $y=0.02$ is about 20%, which is very close to the percolation threshold value as predicted theoretically in 3D percolation model.⁴² In the field range of $0.5 \text{ T} < H < 4 \text{ T}$, there occurs stepwise behavior which is typical for a bulk antiferromagnet. Further increasing the field to $H=6.0 \text{ T}$, M exhibits another sharp increase

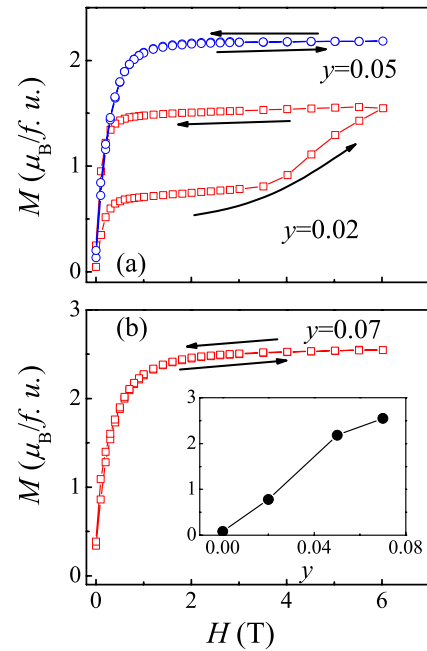


FIG. 4. (Color online) Measured magnetization as a function of H at $T=5 \text{ K}$ for samples of (a) $y=0.02$ and $y=0.05$; and (b) $y=0.07$, respectively. The arrows indicate the cycle of H varying during measurements. The inset of (b) presents the y dependence of magnetization at $T=5 \text{ K}$ and $H=3 \text{ T}$.

which can be ascribed to the field-induced enhancement of FM phase at the expense of CO-AFM matrix. Similar to the M - H behavior of sample $y=0.02$, samples $y=0.05$ and $y=0.07$ all exhibit saturated magnetization achieved at $H=1.0 \text{ T}$, but no more M - H hysteresis can be observed. The saturated M calculated at $H=3 \text{ T}$ continuous increases as y increases from 0 to 0.07, as shown in the inset of Fig. 4(b).

D. Discussion

The transport and magnetization data now allow us to correlate the $\rho(T)$ curve with $M(T)$ curve for sample $y=0.02$ where the PS state is favored. The two curves vary in opposite ways, typical for PS manganites. The conduction is contributed from the CO insulating phase and FM metallic phase, and a percolation transition from insulator to metal arises when the FM metallic phase volume fraction is larger than a critical value.⁴¹ For a detailed investigation, the H dependence of ρ at $T=5 \text{ K}$ for sample $y=0.02$ was measured, shown in Fig. 5. Distinctly, the $\rho(H)$ and $M(H)$ curves evolve in an exactly opposite way. In the low H range, the magnetic field promotes the parallel alignment of FM domains, suppressing the electron-scattering effect by the FM domain walls. Correspondingly, the resistivity exhibits a large decrease. In the field range of $0.5 \text{ T} < H < 4 \text{ T}$, $M(H)$, and $\rho(H)$ both show linear behaviors, indicating the dominant role of FM domain walls in compensation of the CO phase. Further increase in H melts away the CO phase into the FM metallic one, giving rise to another abrupt increase in M and a large decrease in ρ .

In the qualitative sense, we again address that the Ru-doping is extremely powerful in destroying the long-range

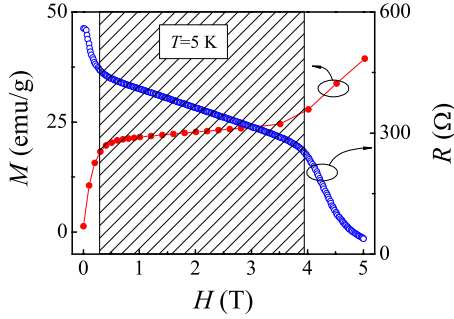


FIG. 5. (Color online) Magnetization (close circle) and resistivity (open circle) as a function of magnetic field H of sample $y=0.02$ at $T=5$ K.

CO state and generating the FM phase in highly stabilized $\text{La}_{0.4}\text{Ca}_{0.6}\text{MnO}_3$. The CMR effect associated with the PS state in sample $y=0.02$ is confirmed and the physics, predicted by Şen *et al.*, that the coexistence and competition between FM metal and CO-AFM insulated phase can cause a true CMR effect, is also well illustrated in samples $y=0.05$ and 0.07 where the CO phase is almost fully suppressed and the FM metallic phase dominated.^{36,37}

At last, we perform a Monte Carlo simulation on the Ru-doping effects using the two-orbital double-exchange model. The details of model Hamiltonian and numerical technique can be found in our previous publication.³⁵ Comparing with the calculation in Ref. 35, two changes: (1) the FM exchange between the Ru and Mn cations^{18–21} and (2) the different e_g electron density have been taken into account to match our experimental material. Despite these two differences, similar results have been obtained. For an instance, the Monte Carlo snapshots of spin configuration at $y=0.031$ and $y=0.064$ are shown in Figs. 6(a) and 6(b), respectively. In Fig. 6(a), some FM clusters can be observed with some remnant short-ranged CE chains. For $y=0.064$ [Fig. 6(b)], there is no trace of any CE order anymore, and the lattice is occupied by the FM domains. These calculated results essentially support our experimental results and the fundamental reason for the CE/CO destabilization and FM phase generation upon the Ru doping can be understood in two aspects. For the first aspect, the Ru cations couple ferromagnetically with Mn ions,^{18–21} which will destroy the AFM interchain coupling in the CE pattern with only some short-ranged CE chains left in the lattice [Fig. 6(a)]. For the second aspect, the doping of Ru cations will enhance the local e_g electron density, which favors the FM phase.^{18,35} Therefore, both of the above factors are responsible for the collapse of the long-range CO-AFM insulated state and hence promote the FM metallic state. Detailedly, for the tiny substituted sample $y=0.02$, the long-range CO-AFM ordering is destroyed and the local e_g electron density is increased for the high valence of Ru cations,

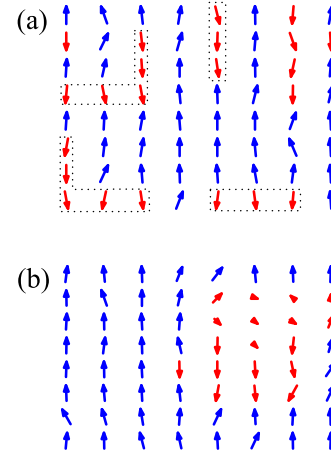


FIG. 6. (Color online) Typical Monte Carlo snapshots of the spin configuration. (a) $y=0.031$ and (b) $y=0.063$. The CE-type spin orders are indicated using dot squares in (a).

giving rise to the generation of FM phase around Ru rich regions. While due to the low concentration of Ru cations, part of the CO-AFM insulated phase still exists and competes with the FM metal, resulting in the PS state as well as the CMR effect. Further increase y , the FM volume fraction continuously increases at the expense of the CO-AFM matrix and reaches a critical point around $y=0.05$, where the CO-AFM insulated phase is almost fully suppressed [Fig. 6(b)].

IV. CONCLUSION

In conclusion, the effect of B -site doping on physical properties of CO-AFM manganites $\text{La}_{0.4}\text{Ca}_{0.6}\text{MnO}_3$ has been investigated using various experimental techniques and theoretical calculation. The results reveal that the robust CO-AFM insulated state in the adopted compound can be significantly suppressed and generates a FM metal by tiny Ru doping. The CMR effect associated with the PS state in sample $y=0.02$ confirms the theoretical prediction of Şen *et al.* Combining a theoretical calculation, it is found that the FM coupling between Ru and Mn spins, and the enhancement of e_g electron density are responsible for the generation of the FM metallic phase, while the topological defects cannot be excluded since it always contributes to the instability of charge-ordered state.

ACKNOWLEDGMENTS

This work was supported by the Natural Science Foundation of China under Grant Nos. 50601013 and 50832002, the National Key Projects for Basic Research of China under Grant Nos. 2006CB921802 and 2009CB623303, and the 111 Programme of MOE of China under Grant No. B07026. We thank Y. D. Ye and H. Q. Yu for their help in XRD measurements performed in Modern Analytical Center, Nanjing University, China.

*Corresponding author; liujm@nju.edu.cn

- ¹C. Renner, G. Aeppli, B.-G. Kim, Y.-A. Soh, and S.-W. Cheong, *Nature* (London) **416**, 518 (2002).
- ²E. Dagotto, T. Hotta, and A. Moreo, *Phys. Rep.* **344**, 1 (2001).
- ³Y. Tokura, *Rep. Prog. Phys.* **69**, 797 (2006).
- ⁴K. F. Wang, Q. Xiao, H. Yu, M. Zeng, M. F. Zhang, and J.-M. Liu, *J. Magn. Magn. Mater.* **285**, 130 (2005).
- ⁵S. Dong, C. Zhu, Y. Wang, F. Yuan, K. F. Wang, and J.-M. Liu, *J. Phys.: Condens. Matter* **19**, 266202 (2007).
- ⁶S. Dong, H. Zhu, and J.-M. Liu, *Phys. Rev. B* **76**, 132409 (2007).
- ⁷K. F. Wang, F. Yuan, S. Dong, D. Li, Z. D. Zhang, Z. F. Ren, and J.-M. Liu, *Appl. Phys. Lett.* **89**, 222505 (2006).
- ⁸D. Akahoshi, M. Uchida, Y. Tomioka, T. Arima, Y. Matsui, and Y. Tokura, *Phys. Rev. Lett.* **90**, 177203 (2003).
- ⁹K. F. Wang, Y. Wang, L. F. Wang, S. Dong, D. Li, Z. D. Zhang, H. Yu, Q. C. Li, and J.-M. Liu, *Phys. Rev. B* **73**, 134411 (2006).
- ¹⁰K. F. Wang, Y. Wang, L. F. Wang, S. Dong, H. Yu, Q. C. Li, J.-M. Liu, and Z. F. Ren, *Appl. Phys. Lett.* **88**, 152505 (2006).
- ¹¹S. Dong, F. Gao, Z. Q. Wang, J.-M. Liu, and Z. F. Ren, *Appl. Phys. Lett.* **90**, 082508 (2007).
- ¹²Z. Q. Wang, F. Gao, K. F. Wang, H. Yu, Z. F. Ren, and J.-M. Liu, *Mater. Sci. Eng., B* **136**, 96 (2007).
- ¹³C. L. Lu, K. F. Wang, S. Dong, J. G. Wan, J.-M. Liu, and Z. F. Ren, *J. Appl. Phys.* **103**, 07F714 (2008).
- ¹⁴A. Banerjee, K. Mukherjee, K. Kumar, and P. Chaddah, *Phys. Rev. B* **74**, 224445 (2006).
- ¹⁵Y. Moritomo, K. Murakami, H. Ishikawa, M. Hanawa, A. Nakamura, and K. Ohoyama, *Phys. Rev. B* **69**, 212407 (2004).
- ¹⁶K. Pradhan, A. Mukherjee, and P. Majumdar, *Phys. Rev. Lett.* **99**, 147206 (2007).
- ¹⁷C. Martin, A. Maignan, F. Damay, M. Hervieu, B. Raveau, Z. Jirak, G. André, and F. Bourée, *J. Magn. Magn. Mater.* **202**, 11 (1999).
- ¹⁸C. Martin, A. Maignan, M. Hervieu, C. Autret, B. Raveau, and D. I. Khomskii, *Phys. Rev. B* **63**, 174402 (2001).
- ¹⁹V. Markovich, E. Rozenberg, G. Gorodetsky, C. Martin, A. Maignan, M. Hervieu, and B. Raveau, *Phys. Rev. B* **64**, 224410 (2001).
- ²⁰V. Markovich, I. Fita, R. Puzniak, E. Rozenberg, A. Wisniewski, C. Martin, A. Maignan, M. Hervieu, B. Raveau, and G. Gorodetsky, *Phys. Rev. B* **65**, 224415 (2002).
- ²¹J. S. Kim, D. C. Kim, G. C. McIntosh, S. W. Chu, Y. W. Park, B. J. Kim, Y. C. Kim, A. Maignan, and B. Raveau, *Phys. Rev. B* **66**, 224427 (2002).
- ²²S. Hébert, A. Maignan, C. Martin, and B. Raveau, *Solid State Commun.* **121**, 229 (2002).
- ²³T. Kimura, Y. Tomioka, R. Kumai, Y. Okimoto, and Y. Tokura, *Phys. Rev. Lett.* **83**, 3940 (1999).
- ²⁴S. Mori, R. Shoji, N. Yamamoto, T. Asaka, Y. Matsui, A. Machida, Y. Moritomo, and T. Katsufuji, *Phys. Rev. B* **67**, 012403 (2003).
- ²⁵A. Machida, Y. Moritomo, K. Ohoyama, T. Katsufuji, and A. Nakamura, *Phys. Rev. B* **65**, 064435 (2002).
- ²⁶C. Yaicle, C. Frontera, J. L. García-Muñoz, C. Martin, A. Maignan, G. André, F. Bourée, C. Ritter, and I. Margiolaki, *Phys. Rev. B* **74**, 144406 (2006).
- ²⁷B. Raveau, A. Maignan, and C. Martin, *J. Solid State Chem.* **130**, 162 (1997).
- ²⁸S. Xu, Y. Moritomo, A. Machida, K. Ohoyama, and A. Nakamura, *J. Phys. Soc. Jpn.* **72**, 922 (2003).
- ²⁹Y. Moritomo, A. Machida, T. Nonobe, and K. Ohoyama, *J. Phys. Soc. Jpn.* **71**, 1626 (2002).
- ³⁰R. Mahendiran, A. Maignan, S. Hébert, C. Martin, M. Hervieu, B. Raveau, J. F. Mitchell, and P. Schiffer, *Phys. Rev. Lett.* **89**, 286602 (2002).
- ³¹C. Yaicle, B. Raveau, A. Maignan, and M. Hervieu, *Solid State Commun.* **132**, 487 (2004).
- ³²Z. B. Yan, S. Dong, K. F. Wang, C. L. Lu, H. X. Guo, and J.-M. Liu, *J. Appl. Phys.* **104**, 013916 (2008).
- ³³V. Markovich, I. Fita, R. Puzniak, C. Martin, A. Wisniewski, C. Yaicle, A. Maignan, and G. Gorodetsky, *Phys. Rev. B* **73**, 224423 (2006).
- ³⁴R. Mahendiran, B. Raveau, M. Hervieu, C. Michel, and A. Maignan, *Phys. Rev. B* **64**, 064424 (2001).
- ³⁵X. Chen, S. Dong, K. F. Wang, J.-M. Liu, and E. Dagotto, *Phys. Rev. B* **79**, 024410 (2009).
- ³⁶C. Şen, G. Alvarez, and E. Dagotto, *Phys. Rev. Lett.* **98**, 127202 (2007).
- ³⁷R. Yu, S. Dong, C. Şen, G. Alvarez, and E. Dagotto, *Phys. Rev. B* **77**, 214434 (2008).
- ³⁸L. Demko, I. Kezsmarki, G. Mihaly, N. Takeshita, Y. Tomioka, and Y. Tokura, *Phys. Rev. Lett.* **101**, 037206 (2008).
- ³⁹C. L. Lu, S. Dong, K. F. Wang, F. Gao, P. L. Li, L. Y. Lv, and J.-M. Liu, *Appl. Phys. Lett.* **91**, 032502 (2007).
- ⁴⁰L. Ghivelder and F. Parisi, *Phys. Rev. B* **71**, 184425 (2005).
- ⁴¹V. Hardy, A. Wahl, and C. Martin, *Phys. Rev. B* **64**, 064402 (2001).
- ⁴²S. Kirkpatrick, *Rev. Mod. Phys.* **45**, 574 (1973).